PERGAMON

Journal of Atmospheric and Solar-Terrestrial Physics 65 (2003) 1127–1137

Journal of ATMOSPHERIC AND SOLAR-TERRESTRIAL PHYSICS

www.elsevier.com/locate/jastp

Derivation of tropospheric column ozone from the Earth Probe TOMS/GOES co-located data sets using the cloud slicing technique

C. Ahn[a], J.R. Ziemke[b,c,*], S. Chandra[c], P.K. Bhartia[c]

[a] *Science Systems and Applications, Inc., Lanham, MD, USA*

[b] *The University of Maryland, Baltimore County (UMBC) Goddard Earth Sciences and Technology (GEST) Center, Baltimore, MD, USA*

[c] *NASA Goddard Space Flight Center, Code 916, Greenbelt, MD 20771, USA*

Received 25 October 2002; received in revised form 28 May 2003; accepted 10 July 2003

Abstract

A recently developed technique called cloud slicing used for deriving upper tropospheric ozone from the Nimbus 7 total ozone mapping spectrometer (TOMS) instrument combined with temperature-humidity and infrared radiometer (THIR) is not applicable to the Earth Probe TOMS (EP TOMS) because this satellite platform does not have an instrument to measure cloud-top temperatures. For continuing monitoring of tropospheric ozone between 200 and 500 hPa and testing the feasibility of this technique across spacecrafts, EP TOMS data are co-located in time and space with the Geostationary Operational Environmental Satellite (GOES)-8 infrared data for year 2001 and early 2002, covering most of North and South America (45°S–45°N and 120°W–30°W). Results show that the maximum column amounts for the mid-latitudinal sites of the northern hemisphere are found in the March–May season. For the mid-latitudinal sites in the southern hemisphere, the highest column amounts are found in the September–November season with overall seasonal variability smaller than that in the northern hemisphere. The tropical sites show weaker seasonal variability compared to higher latitudes. The derived results for selected sites are cross-validated qualitatively with the seasonality of ozonesonde observations and the results from THIR analyses over the 1979–1984 time period. These comparisons show a reasonably good agreement among THIR, ozonesonde observations, and cloud slicing-derived column ozone. Cloud slicing measurements from TOMS coincide with large-scale convection events, especially in regions of the tropospheric wind jets (around ±30° latitude). In these cases they may not be representative of typical conditions in the atmosphere. Two new variant approaches, high-low cloud slicing and ozone profile derivation from cloud slicing are introduced to estimate column ozone amounts using the entire cloud information in the troposphere. A future satellite platform such as the earth observing system (EOS) Aura with the ozone monitoring instrument (OMI) can provide better statistics of derived ozone because of improved spatial resolution and improved measurements of cloud-top pressures.

Keywords: Tropospheric ozone; Cloud slicing; Earth probe TOMS; GOES

1. Introduction

Satellite remote sensing techniques have been used for studying the global distributions, sources and sinks, transport, and seasonal cycles of tropospheric ozone because the distribution of ozone measurements from ground-based observations are sparse and there exists large spatial and temporal variabilities in tropospheric ozone. The first study by Fishman and Larsen (1987) and subsequent study by Fishman et al. (1990) derived tropospheric column ozone (TCO) by subtracting stratospheric column ozone (SCO) of the stratospheric aerosol and gas experiment (SAGE) from total column ozone of the total ozone mapping

* Corresponding author. Atmospheric Chemistry and Dynamics Branch, NASA Goddard Space Flight Center Code 916, Greenbelt, MD 20771, USA. Fax: +301-614-5903.

E-mail address: ziemke@jwocky.gsfc.nasa.gov (J.R. Ziemke).

1364-6826/$ - see front matter
doi:10.1016/S1364-6826(03)00166-4

spectrometer (TOMS). However, the poor sampling of SAGE data restricting daily coverage only to two (sunrise and sunset) narrow 5–10° latitude bands seriously limits the interpretation of tropospheric column ozone maps from daily to monthly time scales. Although Fishman et al. (1996) and Vukovich et al. (1996) used vertical ozone profiles from the solar backscatter ultraviolet 2 (SBUV 2) instrument for mitigating this problem, significant discrepancies to ground-based measurements were noted because of the nature of the SBUV retrieval algorithm. Fishman and Balok (1999) proposed an improved method by adjusting SBUV data with ozonesonde data for deriving SCO and TCO. A similar approach by Ziemke et al. (1998) was to use assimilated microwave limb sounder (MLS) and halogen occultation experiment (HALOE) SCO measurements for deriving TCO with respect to TOMS measurements of total column ozone. That method enables the determination of daily maps of high spatial coverage. However, these types of residual methods have some limitations such as a mismatch in orbital and sampling characteristics between TOMS and the other instruments and inherent sizable inter-instrument calibration errors in calculated TCO.

For overcoming these limitations, Hudson and Thompson (1998) proposed a modified residual method to derive TCO from TOMS measurements and ozonesonde climatology in the tropics without other satellite measurements. This technique assumes a zonally invariant stratospheric component and a tropospheric component consisting of a constant background and a zonally varying wave number 1 structure. The zonally invariant structure of tropical SCO was first described by Fishman and Larsen (1987) using SAGE data and later by Ziemke et al. (1996) using Upper Atmosphere Research Satellite (UARS) MLS data.

Ziemke et al. (1998) introduced the convective-cloud-differential (CCD) method to derive TCO using only TOMS measurements. In the CCD method, SCO from nearby column ozone amounts above the tops of very high tropopause-level clouds under conditions of high reflectivity ($R > 0.9$) are subtracted from total column ozone from low reflectivity ($R < 0.2$) scenes to derive TCO. This technique is also based on the assumption of a zonal invariance of SCO in the tropics as determined from independent SAGE, MLS, and HALOE measurements.

Jiang and Yung (1996) and Newchurch et al. (2001a) used the topographic contrast method (TCM) for deriving long time series of lower tropospheric column ozone. This method subtracted TOMS total column ozone over a mountain region from nearby sea-level TOMS total column ozone. An assumption with this technique is that column ozone above mountain-top altitude is the same over the two geographical regions.

Previous methods are only useful for deriving TCO under some assumptions and in limited regions such as the tropics and mountain regions. Ziemke et al. (2001) introduced a different technique called "Cloud Slicing" to derive upper tropospheric ozone amount given coincident Nimbus-7 measurements of both temperature humidity and infrared radiometer (THIR) cloud-top pressure and TOMS above-cloud column ozone. The method was applied to the low-latitude tropics (15°S–15°N) for years 1979–1984. Because the TOMS instrument measures backscattered ultraviolet wavelength radiation, it cannot detect ozone lying below dense water vapor clouds. This opaque property of clouds can be used directly in conjunction with co-located cloud-top pressure data to derive ozone profile information in the troposphere.

The pilot study of Ziemke et al. (2001) showed promising results to distinguish between upper and lower tropospheric column ozone by combining upper tropospheric column ozone with CCD-derived TCO. More recently, Ziemke et al. (2003) expanded the cloud slicing method to latitudes 60°S to 60°N for 1979–1984 using the Nimbus 7 data. The current Earth Probe TOMS (EP TOMS) satellite platform does not have an instrument to provide in situ cloud-top pressure information like Nimbus 7 THIR. This study tests the feasibility of deriving upper tropospheric ozone from cloud slicing beyond the Nimbus-7 era by collocating ozone from EP TOMS and cloud temperatures from the geostationary operational environmental satellite (GOES) for 2001 and early 2002.

In Section 2 we will explain how GOES data are archived and co-located in time and space with EP TOMS. In Section 3 the derived results for selected sites will be compared with ozonesonde measurements and results from THIR for 1979–1984, and two new variant approaches will be proposed to extend the capability of cloud slicing over the entire troposphere. In Section 3 we also examine the implications of improved spatial resolution from the ozone monitoring instrument (OMI, launch 2004) on increasing the number of measurements from cloud slicing. Finally, Section 4 provides a summary.

2. Data and methodology

The GOES-8 spacecraft launched on April 13, 1994 is operational as GOES-EAST at 75°W and provides imagery for monitoring weather conditions such as tornadoes, flash floods, hail storms, and hurricanes. It circles the Earth in a geosynchronous orbit, which means it orbits the equatorial plane of the Earth at a speed matching the Earth's rotation. This allows it to hover continuously over one position on the surface. The geosynchronous plane is about 35,800 km (22,300 miles) above the Earth, high enough to allow a full-disc view of the Earth (http://www.oso.noaa.gov/goes/index.htm). GOES-8 data from infrared channel 4 (11 μm) were selected to be co-located with EP TOMS for the consistency of data analyses of Nimbus-7 THIR. GOES has nearly the same spectral channel as 10.5–12.5 μm (11.5 μm mean) of THIR to provide cloud-top temperatures. GOES provides high frequency of data at every 15 min increment that enables

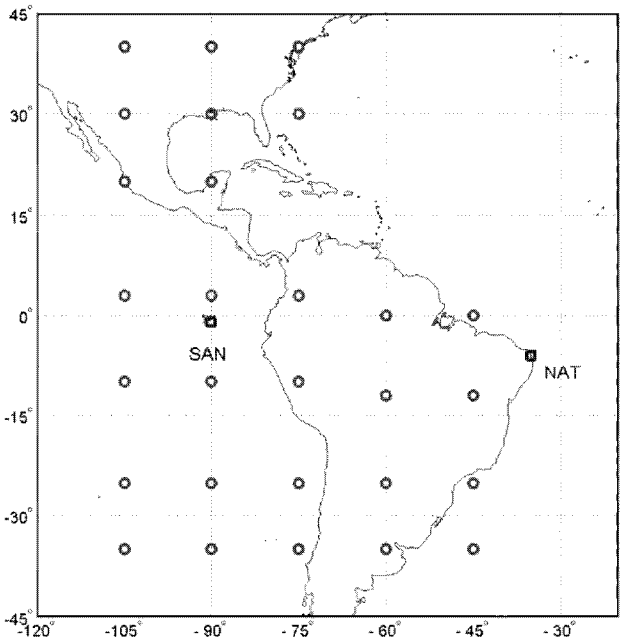

Fig. 1. EP TOMS/GOES-8 co-located sites of 30 over 5 GOES sectors, including 'Conus', 'Galapagos', 'Brazil', 'Easter', and 'Argentina'. Two ozonesonde stations are represented as square marks on the San Cristobal (SAN) and Natal (NAT) sites, respectively. Others are represented as circles located over each sector as evenly as possible with approximately 15° longitudinal interval.

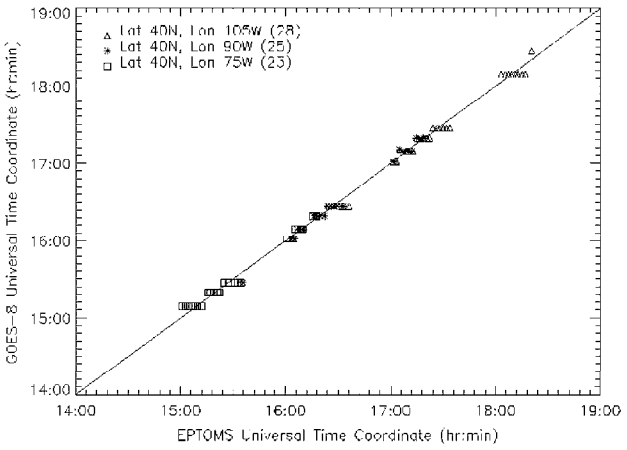

Fig. 2. Time collocation of EP TOMS and GOES-8 for February 2002 at three locations, (40°N, 105°W), (40°N, 90°W), (40°N, 75°W). Numbers in parentheses for each location denote available co-located data sets (days) per month.

us to collocate time and space with EP TOMS without matching orbits of other sun-synchronous satellites such as the EOS-terra moderate resolution imaging spectroradiometer (MODIS), (web site http://modis.gsfc.nasa.gov) and tropical rain measuring mission (TRMM), (web site http://trmm.gsfc.nasa.gov).

Brightness temperature from GOES infrared channel is converted to 1-byte grayscale in 256 steps 0.5 K wide, downward from 320 to 192 K and stored as a tag image file format (TIFF) (web site http://rsd.gsfc.nasa.gov/). These GOES-8 TIFF files were automatically downloaded from this web site with a large time window of nine universal time coordinate (UTC) through 22 UTC over five sectors covering most of North/South America and adjacent oceans for a year period from March of 2001 through the end of February of 2002. Each sector is centered on and named after a geographical region, such as 'Conus', 'Brazil', 'Galapagos', 'Easter', and 'Argentina'. A more detailed information of GOES data can be obtained from the web site above.

Fig. 1 shows 30 co-located study sites including two ozonesonde stations, in San Cristobal and Natal. These sites were selected as evenly spaced over each limited geographic sector as possible when 5° × 5° bins are used to make the ensemble statistics of above-cloud ozone and cloud-top pressure.

A precise collocation task is the most crucial step to do cloud slicing with combined EP TOMS/GOES data sets. Prior to spatial collocation, a median UTC (hour: minute: second) of EP TOMS was computed from the EP TOMS Greenwich Mean Time (in second of day at start of scan) record using a 3° × 3° bin over the center of each site and a GOES TIFF file with corresponding time stamp within 30 min was found from the GOES archive directory. Fig. 2 shows time collocations of 3 longitudes (105°W, 90°W, and 75°W) at 40°N for February 2002. The EP TOMS coverage for one cross-track corresponds to about 20° longitude at the equator with 4° missing orbit, and thus it takes about 15 orbits per day to cover the entire globe. The nadir track shifts about 10° eastward each day. Therefore, the orbits at 40°N are slightly overlapped. These orbital time differences of EP TOMS are well represented in Fig. 2 by aligning the UTC times of EP TOMS and GOES-8 to a one-to-one line with about 1 hour interval that is approximately equal to 15° of longitude. The numbers in parentheses indicate available co-located data sets (days per month) for each site. Less than 28 co-located data sets implies either missing orbits of EP TOMS or missing GOES files to be co-located. This time-matched GOES file was used for detecting much smaller high resolutions of GOES pixels (4 km × 4 km) analytically at the given EP TOMS instantaneous field of view (IFOV) coordinates. The footprint size of EP TOMS IFOV is dependent on scan angles from 38 km (at nadir) to 200 km (at off-nadir), about 100 km on average. Fig. 3 compares small and large EP TOMS footprints with co-located GOES data points within 5° × 5° bin frames. The number of co-located GOES data within each EP TOMS IFOV is within a range of approximately 60–230 which is proportional to the sizes of nadir and off-nadir EP TOMS IFOV. These results indicate a precise collocation

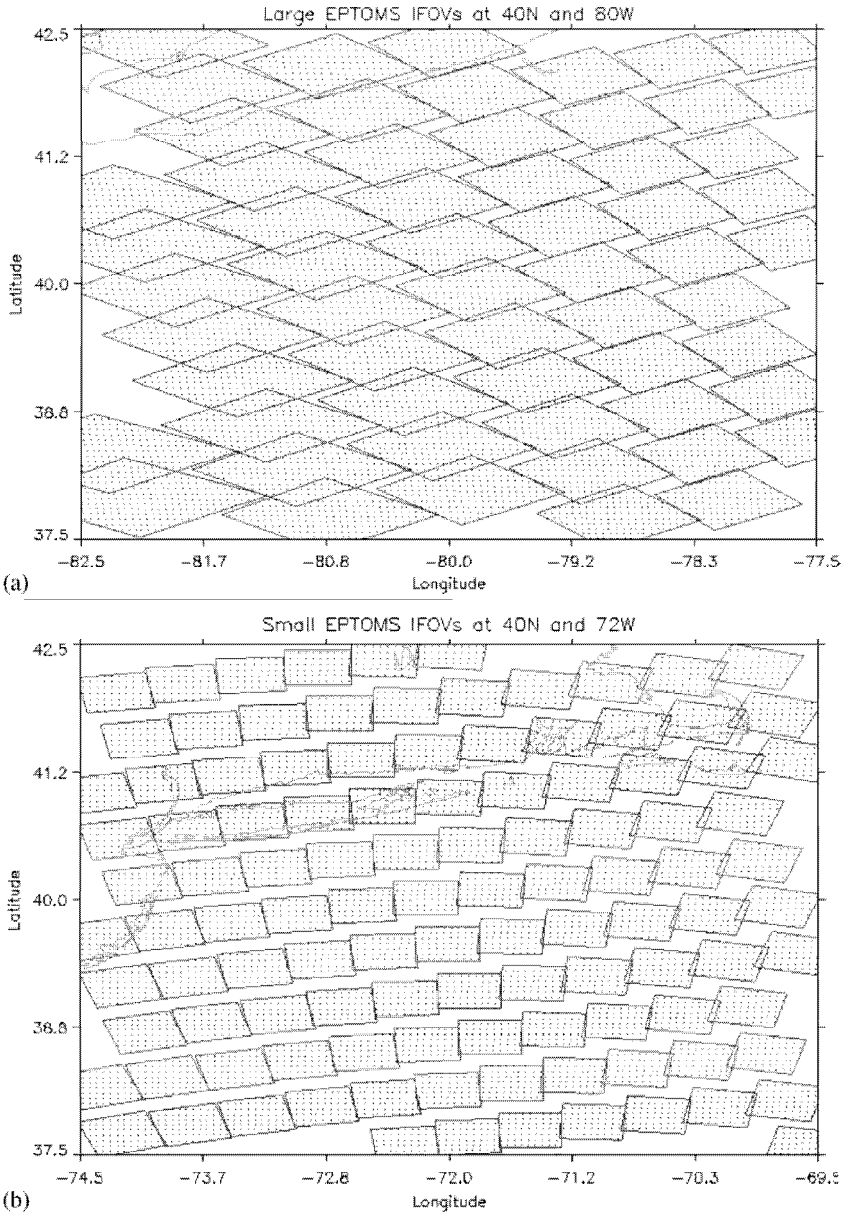

Fig. 3. Comparisons of spatial collocation of EP TOMS and GOES-8 for small and large EP TOMS IFOV coordinate cases within $5° \times 5°$ bins centered at (40°N, 72°W) and (40°N, 80°W), respectively, for February 28, 2002. Polygons are EP TOMS IFOVs, and dots denote relatively fine GOES pixels falling into each EP TOMS IFOV.

of time and space and adequate estimate of cloud-top pressure with enough GOES data for each EP TOMS IFOV.

For deriving the cloud-top pressures from GOES, we used the National Centers for Environmental Prediction (NCEP)/Climate Prediction Center (CPC) meteorological analyses of brightness temperature at 18 pressure levels (0.4–1000 hPa) interpolated to a grid of 5° longitude × 2° latitude (Newman and Nash, 2000).

The NCEP/CPC produces analyses based on the T126 global data assimilation system (GDAS) model with an objective analysis of satellite and radiosonde data. Temperatures and geopotential heights are basic products of this tropospheric–stratospheric hybrid system. More detailed information of the NCEP/CPC analyses generated and maintained by the NASA Goddard Space Flight Center/Code 916 can be obtained from the web site http://code916.gsfc.nasa.gov/Public/Analysis/met/met_analysis.html.

The mean and standard deviation of GOES brightness temperature within EP TOMS IFOV coordinates were computed, and the mean value was converted into a cloud-top pressure using the corresponding NCEP temperature profile.

The procedure for cloud slicing is to make a linear fit between co-located measurements of GOES cloud-top pressure and above-cloud column ozone from EP TOMS over a pre-selected pressure band (200–500 hPa in this study). The mean slope of this linear fit then yields directly the mean volume mixing ratio for ozone within that pressure band. Specifically, mean volume mixing ratio ($\bar{X}$, in ppmv) is determined from

$$\bar{X} = 1.27\Delta\Omega/\Delta P, \quad (1)$$

where Ω is above column ozone (in DU) and P is cloud-top pressure (in hPa). In principle, cloud slicing in this study is the same as the original cloud slicing technique described by Ziemke et al. (2001) except for relaxing some thresholds to increase the available number of ensemble co-measurements over $5^\circ \times 5^\circ$ binned regions per day. EP TOMS footprints scenes with reflectivity greater than 0.4 are used as 100% cloud-filled (i.e., 100% cloud fraction) scenes as shown by Eck et al. (1987) for Nimbus 7 TOMS. This criteria improves the number of measurements when compared to using the 0.6 value of reflectivity by Ziemke et al. (2001). In this study, EP TOMS reflectivity above 0.4 was sufficient for screening 100% cloud-filled scenes (Eck et al., 1987) -as well as increasing the number of cloud pixels per day. The daily minimum number of co-measurements within a $5^\circ \times 5^\circ$ bin is decreased from 20 (as used by Ziemke et al., 2001) to 3. Another threshold applied to daily computed upper tropospheric column ozone (UTO) is to filter out extreme values (greater than 190 ppbv or less than 13 ppbv, which is nearly the same as the 2-sigma filtering rule of Ziemke et al. (2001)). Large variabilities in derived ozone can be generated by strong dynamics associated with wind jets and synoptic-scale baroclinic disturbances. Mesoscale convective complex (MCC) regions can cause an inverse relationship between above-cloud ozone and cloud-top pressure near the tropopause, particularly in the mid latitudes of the northern hemisphere (Poulida et al., 1996). Over clean tropical oceans this convection effect will distribute low ozone air throughout the troposphere regardless of cloud height. These regions may not support the assumption of well-mixed ozone and a hydrostatic atmosphere in the troposphere. Finally, monthly means were computed using at least 3 days per month under these requirements.

Ozonesonde climatology from World Ozone and Ultraviolet Radiation Data Center (WOUDC); (web site http://www.msc-smc.ec.gc.ca/woudc/) and cloud slicing-derived UTO from the Nimbus 7 THIR study is compared with the results from this study for comparison and validation purposes.

3. Results and discussions

In order to demonstrate the linear relationship between cloud-top pressure and above-cloud column ozone, scatter plots for six selected sites in Fig. 4 are constructed using all available co-measurements for the month of March 2001. In each frame in Fig. 4 the first numbers in parenthesis are 2-sigma statistical uncertainties, and the second numbers are the available days per month. The scattering of data in Fig. 4 implies not only potential conversion errors from cloud-top temperature to pressure and errors in EP TOMS above-cloud column ozone, but also true photochemical changes or dynamical perturbations of column ozone. As noted by Ziemke et al. (2001) this follows because the data points for each frame in Fig. 4 are accumulated over an entire month. Because of intense dynamical conditions outside the tropics (i.e., from baroclinic waves, etc.), day-to-day measurements from cloud slicing may be large which makes values derived from monthly ensembles difficult to interpret. Therefore, daily mean volume mixing ratios are derived at all sites and then converted to pseudo-monthly means for making seasonal cycle comparisons.

3.1. Upper tropospheric ozone from cloud slicing

In order to augment the validation of the results from cloud slicing in this study, we refer to the results in Fig. 4 (not shown here) from Ziemke et al. (2003). In that figure, WOUDC ozonesonde climatologies were pre-filtered for low tropopause pressure (less than 200 hPa) and subsequently compared with the results from cloud slicing. The locations of several ozonesonde stations were from mid-to-high latitudes in the northern hemisphere (i.e., US, Europe, Japan) except for Natal (6°S, 35°W) and Aspendale-Laverton (38°S, 145°E) sites. The seasonal cycles and mean amounts in UTO from cloud slicing compared well with ozonesondes with largest UTO in spring months in both hemispheres. However, this seasonal cycle behavior of the mid-latitudinal sites of the northern hemisphere is different from general (i.e., not filtered for higher tropopause) ozonesonde climatology which shows UTO maximizing around early-to-mid summer months. Because of large footprint measurements from TOMS ($\sim$100 km on average), UTO derived from cloud slicing coincides with large-scale convection events. These events are not necessarily representative of average atmospheric conditions in regions near and poleward of the tropospheric wind jets, especially in winter and spring seasons when dynamical wave activity in the troposphere and lower stratosphere is most intense. We note that the seasonal cycle characteristics and spatial patterns in UTO from cloud slicing are similar to lower stratospheric ozone, especially during winter–spring months when derived UTO amounts are largest (Ziemke et al., 2003).

Fig. 5 summarizes the results of derived UTO from cloud slicing as a function of month at four representative sites. In Fig. 5 the results from Nimbus 7 THIR (1979–1984 seasonal cycles) are superimposed for comparing seasonal variabilities. Included in Fig. 5 in each frame are associated 1σ (i.e., one standard deviation) uncertainty bars which for EP TOMS show relatively large errors due to minimum

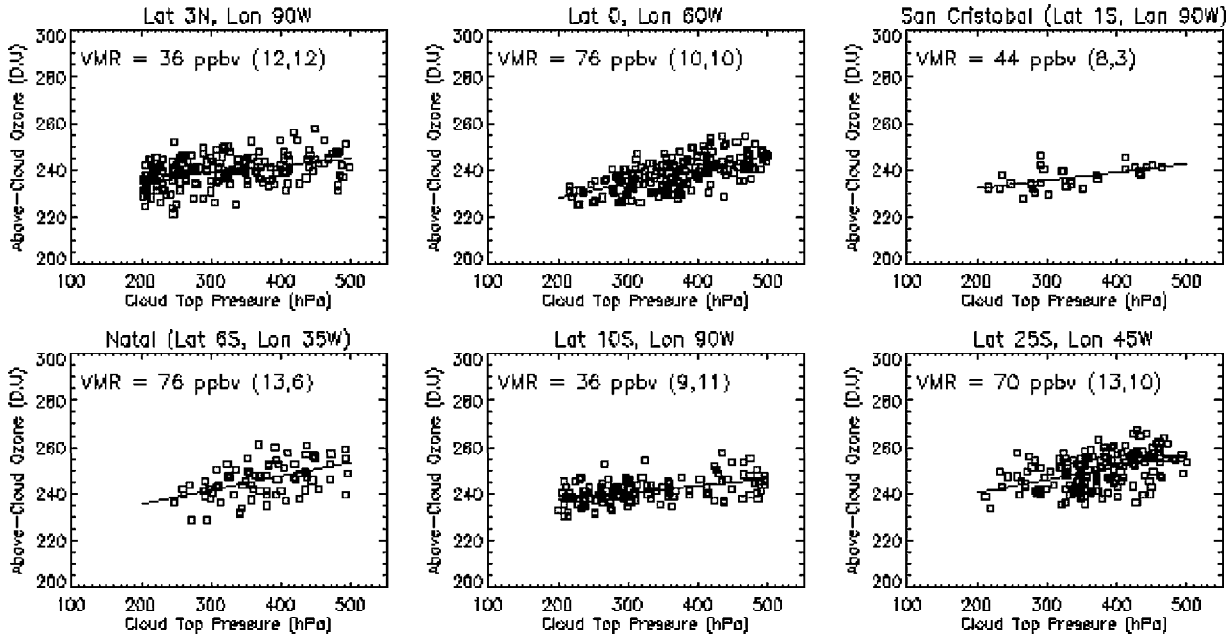

Fig. 4. Scatter plots of above-cloud column ozone versus cloud-top pressure at six study sites for March, 2001. Each frame shows the mean volume mixing ratio (VMR, in ppbv) with 2-sigma uncertainty and available days per month in parenthesis.

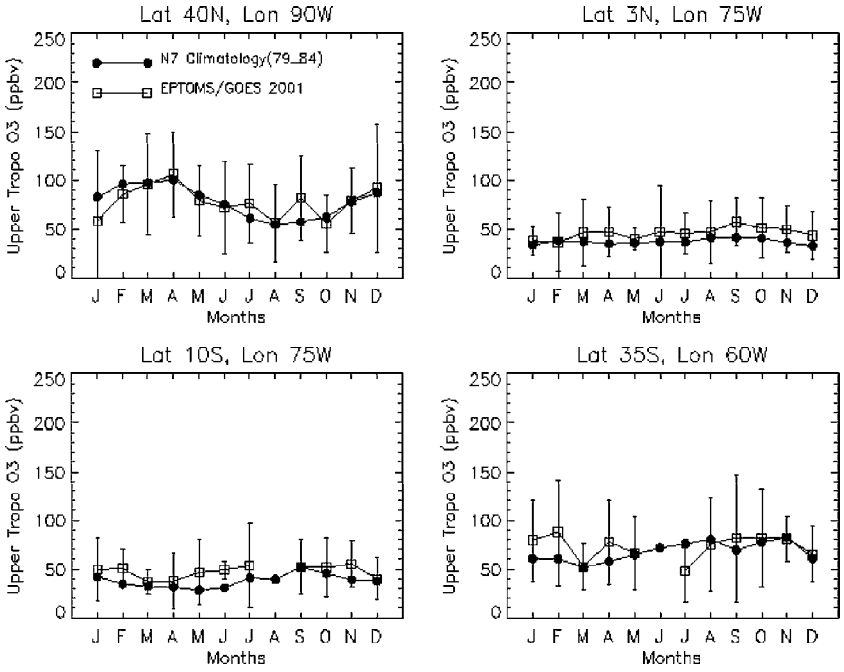

Fig. 5. Derived UTO in the pressure band of 200–500 hPa from cloud slicing at four selected sites using the minimum threshold strategy (three co-measurements, [13 ppbv $\leqslant$ UTO $\leqslant$ 190 ppbv]/day, three measurements/month). Available Nimbus 7 THIR climatology for the 1979–1984 time period is added to the corresponding sites for comparisons. Included are ± 1 standard deviation bars for EP UTO measurements.

samples of three used for computing mean ozone volume mixing ratio per day. The frames in Fig. 5 are arranged from the northern hemisphere (40°N, 90°W) to the southern hemisphere (35°S, 60°W). Values for January and February are for 2002. All other months in Fig. 5 are for year 2001.

In Fig. 5 the largest UTO amounts in the northern hemisphere mid-latitudes occur during winter–spring months, peaking in March–May season. Smallest ozone amounts occur in the fall season (September–October). For the southern hemisphere, these seasonal cycles are reversed with less

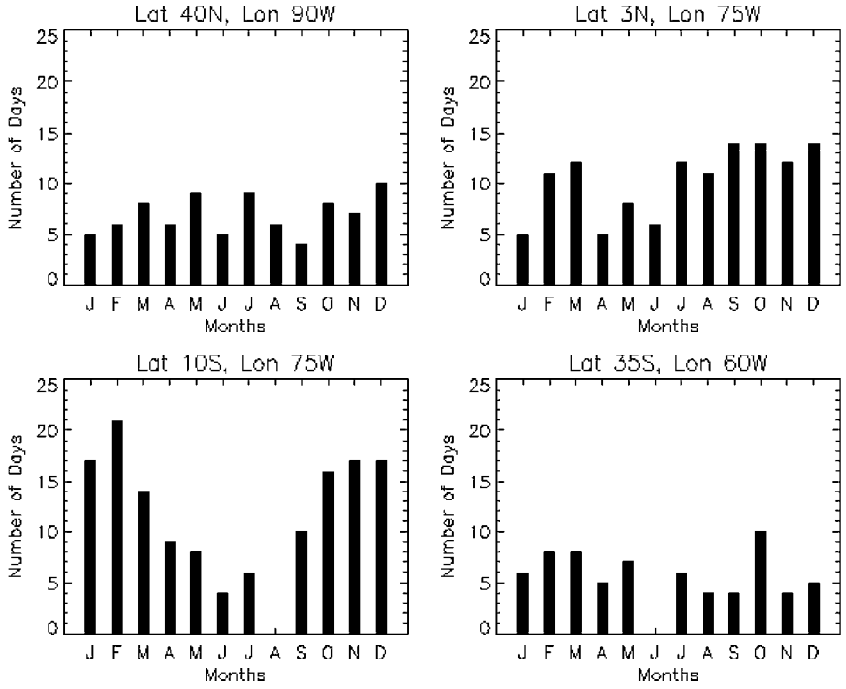

Fig. 6. Number of computed UTO daily measurements per month for making a monthly mean using the minimum threshold strategy (three co-measurements, [13 ppbv $\leqslant$ UTO $\leqslant$ 190 ppbv]/day, three days/month).

variability than those of the northern hemisphere. The tropical sites within $\pm 10^{\circ}$ latitude show a weak seasonal cycle variability and smaller amounts when compared with higher latitudes. Some of the sites do not have sufficient clouds to derive UTO mainly due to dry seasons in the tropics or low marine stratocumulus clouds, usually at altitudes below 700 hPa for all 25°S sites over oceans. These seasonal cycle characteristics and morphology compare well with the results from Nimbus 7 THIR. Fig. 6 shows the number of days used for computing monthly mean UTO from cloud slicing in Fig. 5. The large uncertainty bars in some months in Fig. 5 are caused by a combination of day-to-day variabilities and small number of samples per month (some months in Fig. 6, especially winter–spring months, show five or less samples).

3.2. Mean tropospheric column ozone from high-low (HL) cloud slicing

It may not be enough to filter out partial cloud effects of EP TOMS data using only the reflectivity threshold of 0.4 because the coarse resolution of measurements may result in a biased estimation (over- or underestimation) of above-cloud column ozone. Standard deviations computed from the GOES temperature-to-cloud-top pressure conversion process within each EP TOMS IFOV are used as a threshold to filter out broken clouds in terms of spatial statistics. Fig. 7 shows scatter plots of standard deviations of GOES brightness temperature versus cloud-top pressures for six sites using 5-month composite data (e.g., March–July 2001). Low standard deviation values indicate relatively homogeneous EP TOMS IFOV representing optically thick clouds. These results show that optically thick clouds are usually found from low pressure around 150–250 hPa and high pressure around 700–800 hPa rather than at intermediate pressure levels. Intermediate pressure levels around 400–600 hPa are where most multi-layer broken clouds exist.

We introduce a variant approach called HL cloud slicing based on these findings to extend derived TCO below 500 hPa by using available low cloud height information. Fig. 8 shows the results of derived TCO in the pressure band of 200 (center of high clouds, 150–250 hPa)–750 hPa (center of low clouds, 700–800 hPa). In Fig. 8 six sites were chosen for April 2001. Before fitting the clusters around 200 hPa and 750 hPa, the data above standard deviation of 5 K were removed to use only spatially homogeneous data (assuming optically thick clouds). Latitudinal gradients of derived TCO amounts (in ppbv) from HL cloud slicing are well represented in Fig. 8 from high-to-low latitudes except for a site at 30°N and 105°W. HL cloud slicing might be a promising approach to derive TCO for the pressure band between 200 and 750 hPa, particularly in mid/high latitudes where there exists a sufficient number of coincident high and low clouds.

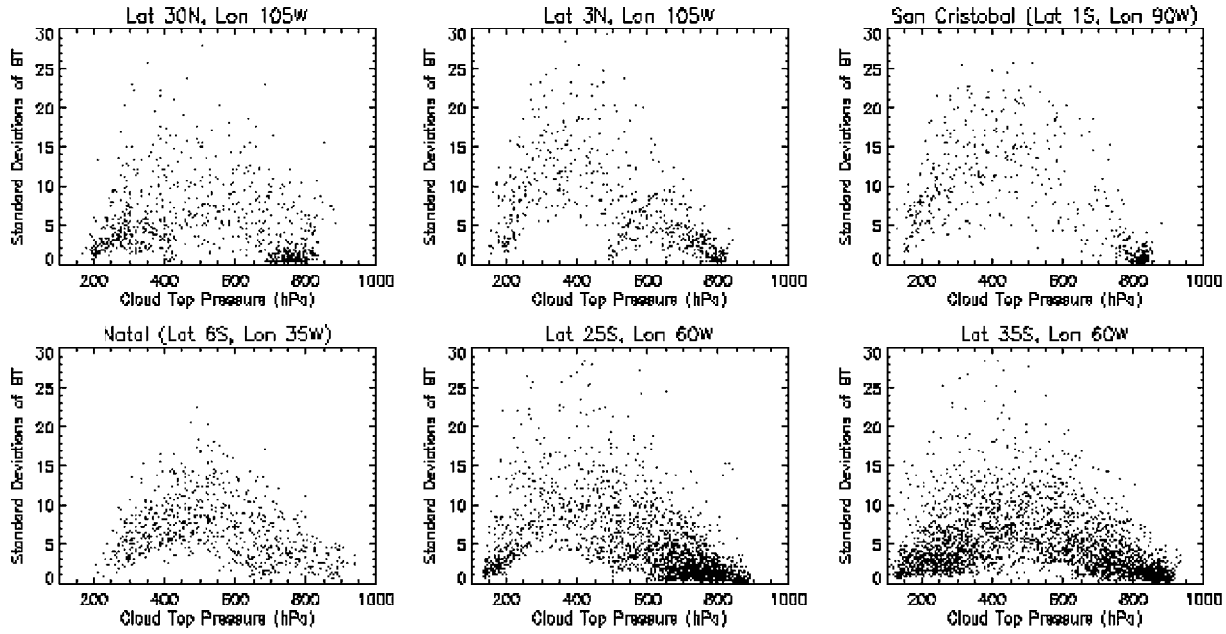

Fig. 7. Scatter plots of standard deviations of GOES brightness temperatures within each EP TOMS IFOV as a function of cloud-top pressure from 5 months (March–July, 2001) of co-measurement data.

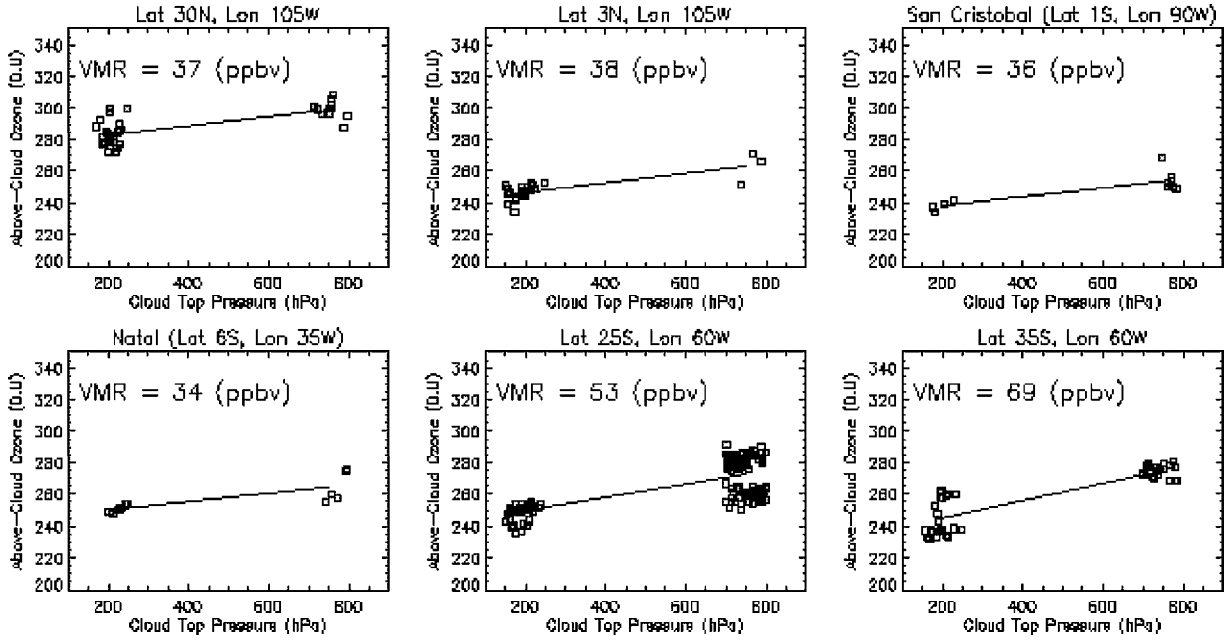

Fig. 8. UTO derived from HL cloud slicing at six selected sites for April, 2001. UTO was derived by fitting the data clusters around 200 and 750 hPa (see text).

3.3. *Ozone profiles derived from cloud slicing*

Ozone profile information can be constructed from cloud slicing if concurrent measurements of clear-sky total column ozone are available. The Natal site (6°S, 35°W) was selected to show a potential use of cloud slicing for deriving ozone profile information. This site has sufficient clouds representing a good linear relationship of cloud-top pressure and above-cloud ozone for cloud heights from 200 hPa through 800 hPa. Fig. 9 shows the comparisons of ozone profiles from cloud slicing and WOUDC climatology for April and June 2001. Cloud-top pressures are converted to

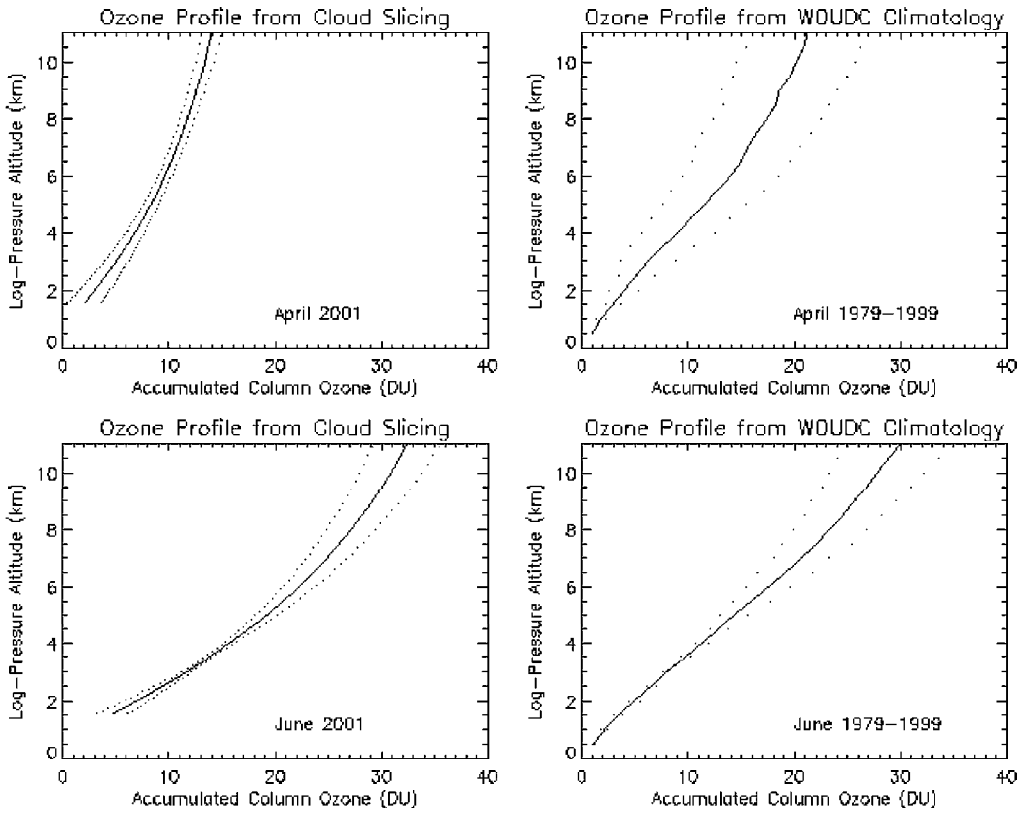

Fig. 9. Comparisons at Natal (6°S, 35°W) of ozone profiles from cloud slicing for 2001 and 1979–1999 WOUDC ozonesonde climatology for April (top frames) and June (bottom frames). Dotted curves designate ±1 standard deviations.

logarithm-scale standard altitude (in km, using a scale height of 7 km). Therefore, cloud-top pressure of 200 hPa is nearly equal to 11 km, and 800 hPa about 1.6 km.

Accumulated column ozone is computed by subtracting above-cloud column ozone at a given pressure level from a virtual clear-sky total column ozone. The virtual total column amount is calculated by extrapolating the cloud slicing linear fit to a near-boundary layer pressure of 900 hPa. The above-cloud column ozone amount at 900 hPa (~700 m altitude) then becomes the virtual total column ozone value. It is assumed that the contribution from ozone below this altitude is zero.

In general, the TOMS retrieved ozone amounts above clouds tend to be overestimated due to the increased multiple scattering inside clouds and between multi-layer clouds. It is possible for errors to exceed several DU (e.g., Newchurch et al., 2001b). The overestimation is greater for clouds lying in the lower troposphere because of increased photon-absorption path lengths (Hudson et al., 1995; Kurosu et al., 1997; Mayer et al., 1998; Newchurch et al., 2001b; Thompson et al., 1993). Therefore, the back-scattered radiation from cloudy scenes, particularly for clouds in the lower troposphere is a complicated process of reduced probability of photons reaching TOMS detectors due to strong Rayleigh scattering at UV wavelengths (i.e., poor retrieval efficiency) and enhanced absorption path length (particularly when high ozone amounts exist inside clouds). Unfortunately, the current opaque Lambertian reflecting model of the EP TOMS algorithm does not fully explain the enhanced ozone above clouds. Errors in the estimated ozone amounts above the mid-to-lower altitude clouds may cause a steeper slope of the cloud slicing linear fit, resulting in large errors in derived ozone profile information in the lower troposphere (i.e., below 5 km) when compared to those from WOUDC. In Fig. 9, summer (June) season is consistently higher, ~10 DU in the upper troposphere than spring season (April) for both cloud slicing and WOUDC ozonesondes. The derived ozone profiles from cloud slicing are comparable to ozonesondes within the standard deviation ranges of WOUDC.

3.4. *Implications for future EOS aura*

The OMI on the EOS aura satellite platform scheduled for launch in 2004 will provide greater spectral and spatial resolution (around 13 km × 24 km at nadir) compared to EP TOMS. Cloud-top pressure can be measured directly using the molecular oxygen "dimer" (O_2–O_2) method (Acarreta and de Haan, 2001) and the rotational Raman scattering

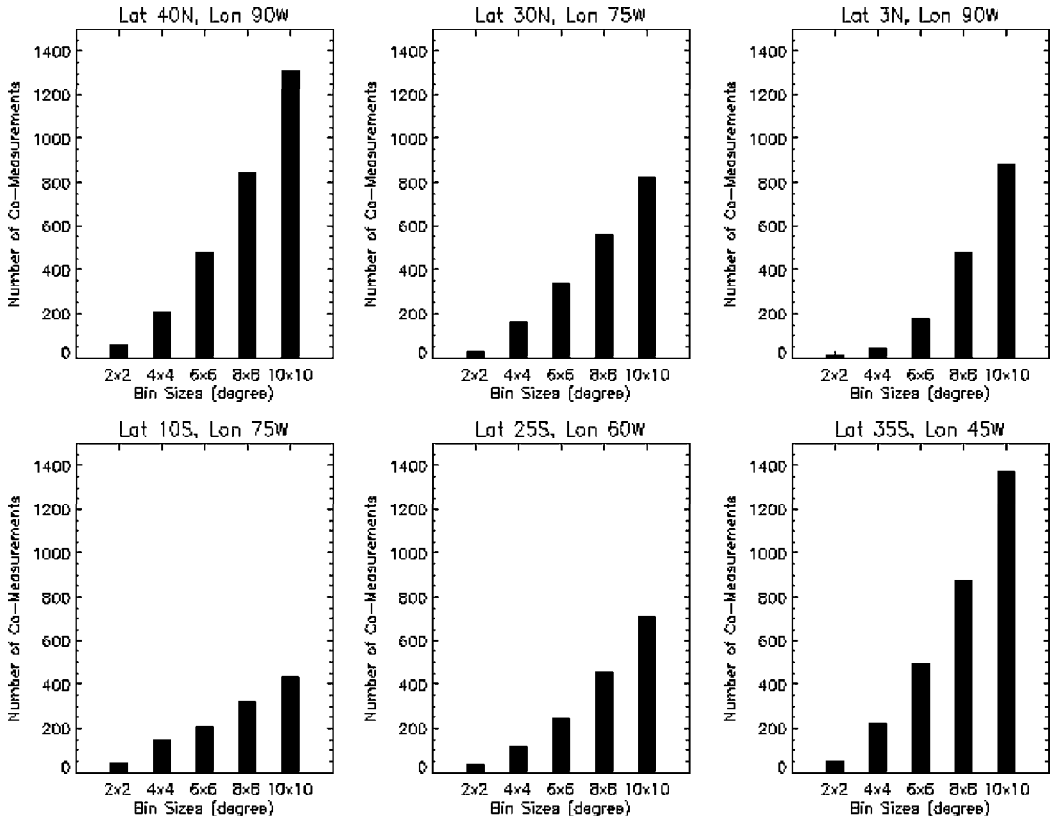

Fig. 10. Number of cumulative co-measurements at six selected sites for August 1980 by changing bin size from ($2^\circ \times 2^\circ$) through ($10^\circ \times 10^\circ$). Data analyzed: Nimbus 7 THIR. Figure illustrates the effects of improved spatial resolution on the increase of sample size.

"Ring Effect" (Joiner and Bhartia, 1995) without having to first convert cloud-top temperature to cloud-top pressure using meteorological analyses. Under the assumption of fractal geometry of clouds (i.e., similar clouds are randomly scattered and independent of the size of IFOV, at least in a limited range of scales), the effects of increased spatial resolution of future OMI on the number of co-measurements can be simulated. This is done (Fig. 10) by increasing bin sizes over six selected locations with the Nimbus 7 THIR data for August 1980. The OMI spatial resolution is at least 5 times better than the EP TOMS at nadir position (i.e., about $5 = (38\ \text{km} \times 38\ \text{km})/(13\ \text{km} \times 24\ \text{km})$). The number of co-measurements is exponentially increased from $2^\circ \times 2^\circ$ bins through $10^\circ \times 10^\circ$ bins for most all of the locations. As a result, the increased samples of co-measurements and a reduced bin size (e.g., smaller than the current $5^\circ \times 5^\circ$ binning for EP TOMS) will provide improved results from cloud slicing.

4. Summary

This is the first study demonstrating that cloud slicing can be accomplished for deriving tropospheric ozone information using ozone and cloud measurements from independent satellite instruments. Previous cloud slicing analyses relied on using a single-satellite platform for these measurements. Cloud slicing was accomplished by collocating EP TOMS and GOES-8 in space and time for the year 2001 and early 2002. UTO was derived for the 200–500 hPa pressure band with coverage over most of North and South America (e.g., 45°S–45°N and 120°–30°W). Outside the tropics, maximum UTO occurs during the spring months in both hemispheres. In the tropics the seasonal cycle variabilities were found to be weak compared to higher latitudes. HL cloud slicing and ozone profiling introduced in this study are innovative applications of cloud slicing with entire cloud information in the troposphere used for inferring ozone amounts. These proposed new techniques of HL cloud slicing and ozone profile derivation will also take advantage of the improved estimation of cloud-top pressure and above-cloud ozone from upcoming OMI. The improved spatial resolution of OMI will enable us to obtain more robust statistics of UTO derived from cloud slicing by increasing the number of co-measurements within a bin at a given site. A further study to refine and optimize thresholds of cloud slicing approaches is still needed to better understand the relationships of cloud-top pressure and above-cloud ozone amounts with respect to the temporal and spatial variability of tropospheric ozone.

Acknowledgements

We wish to thank Dave Larko for extensive help in obtaining GOES data. We also wish to thank the two anonymous reviewers for helpful comments for improving this manuscript.

References

Acarreta, J.R., de Haan, J.F., 2001. Cloud pressure algorithm based on O_2–O_2 absorption. In: Stammes, P. (Ed.), OMI Algorithm Theoretical Basis Document, NASA, Vol. 3. pp. 17–29.

Eck, T.F., Bhartia, P.K., Hwang, P.H., Stowe, L.L., 1987. Reflectivity of Earth's surface and clouds in ultraviolet from satellite observations. Journal of Geophysical Research 92, 4287–4296.

Fishman, J., Balok, A.E., 1999. Calculation of daily tropospheric ozone residuals using TOMS and empirically improved SBUV measurements: application to an ozone pollution episode over the eastern United States. Journal of Geophysical Research 104, 30,319–30,340.

Fishman, J., Larsen, J.C., 1987. Distribution of total ozone and stratospheric ozone in the tropics: implications for the distribution of tropospheric ozone. Journal of Geophysical Research 92, 6627–6634.

Fishman, J., Watson, C.E., Larsen, J.C., Logan, J.A., 1990. Distribution of tropospheric ozone determined from satellite data. Journal of Geophysical Research 95, 3599–3617.

Fishman, J., Brackett, V.G., Browell, E.V., Grant, W.B., 1996. Tropospheric ozone derived from TOMS/SBUV measurements during TRACE A. Journal of Geophysical Research 101, 24,069–24,082.

Hudson, R.D., Thompson, A.M., 1998. Tropical tropospheric ozone (TTO) from TOMS by a modified-residual method. Journal of Geophysical Research 103, 22,129–22,145.

Hudson, R.D., Kim, J-H., Thompson, A.M., 1995. On the derivation of tropospheric column ozone from radiances measured by the total ozone mapping spectrometer. Journal of Geophysical Research 100, 11,137–11,145.

Jiang, Y., Yung, Y.L., 1996. Concentrations of tropospheric ozone from 1979 to 1992 over tropical Pacific South America from TOMS data. Science 272, 714–716.

Joiner, J., Bhartia, P.K., 1995. The determination of cloud pressures from rotational Raman scattering in satellite backscatter ultraviolet measurements. Journal of Geophysical Research 100, 23,019–23,026.

Kurosu, T., Rozanov, V.V., Burrows, J.P., 1997. Parameterization schemes for terrestrial water clouds in the radiative transfer model GOMETRAN. Journal of Geophysical Research 102, 21,809–21,823.

Mayer, B., Kylling, A., Madronich, S., Seckmeyer, G., 1998. Enhanced absorption of UV radiation due to multiple scattering in clouds: experimental evidence and theoretical explanation. Journal of Geophysical Research 103, 31,241–31,254.

Newchurch, M.J., Liu, X., Kim, J.H., 2001a. Lower-tropospheric ozone (LTO) derived from TOMS near mountainous regions. Journal of Geophysical Research 106, 20,403–20,412.

Newchurch, M.J., Liu, X., Kim, J.H., Bhartia, P.K., 2001b. On the accuracy of TOMS retrievals over cloudy regions. Journal of Geophysical Research 106, 32,315–32,326.

Newman, P.A., Nash, E.R., 2000. Quantifying the wave driving of the stratosphere. Journal of Geophysical Research 105, 12,485–12,497.

Poulida, O., Dickerson, R.R., Heymsfield, A., 1996. Stratosphere–troposphere exchange in a midlatitude mesoscale convective complex 1. Observations. Journal of Geophysical Research 101, 6823–6836.

Thompson, A.M., McNamara, D.P., Pickering, K.E., McPeters, R.D., 1993. Effect of marine stratocumulus on TOMS ozone. Journal of Geophysical Research 98, 23,051–23,057.

Vukovich, F.M., Brackett, V., Fishman, J., Sickles II, J.E., 1996. On the feasibility of using the tropospheric ozone residual (TOR) for non-climatological studies on a quasi-global scale. Journal of Geophysical Research 101, 9093–9105.

Ziemke, J.R., Chandra, S., Thompson, A.M., McNamara, D.P., 1996. Zonal asymmetries in southern hemisphere column ozone: implications for biomass burning. Journal of Geophysical Research 101, 14,421–14,427.

Ziemke, J.R., Chandra, S., Bhartia, P.K., 1998. Two new methods for deriving tropospheric column ozone from TOMS measurements: the assimilated UARS MLS/HALOE and convective-cloud differential techniques. Journal of Geophysical Research 103, 22,115–22,127.

Ziemke, J.R., Chandra, S., Bhartia, P.K., 2001. Cloud slicing: a new technique to derive upper tropospheric ozone from satellite measurements. Journal of Geophysical Research 106, 9853–9867.

Ziemke, J.R., Chandra, S., Bhartia, P.K., 2003. Upper tropospheric ozone derived from cloud slicing technique: implications for large-scale convection. Journal of Geophysical Research, 108 (D13), 4390, 10.1029/2002JD002919.